In vivo evaluation of physiologic control algorithms for left ventricular assist devices based on left ventricular volume or pressure

Ochsner, Gregor ; Wilhelm, Markus J ; Amacher, Raffael ; Petrou, Anastasios ; Cesarovic, Nikola ; Staufert, Silvan ; Röhrnbauer, Barbara ; Maisano, Francesco ; Hierold, Christofer ; Meboldt, Mirko ; Schmid Daners, Marianne

Abstract: Turbodynamic left ventricular assist devices (LVADs) provide a continuous flow depending on the speed at which the pump is set, and do not adapt to the changing requirements of the patient. The limited adaptation of the pump flow (PF) to the amount of venous return can lead to ventricular suction or overload. Physiologic control may compensate such situations by an automatic adaptation of the PF to the volume status of the left ventricle. We evaluated two physiologic control algorithms in an acute study with eight healthy pigs. Both controllers imitate the Frank-Starling law of the heart and are based on a measurement of the left ventricular volume (LVV) or pressure (LVP), respectively. After implantation of a modified Deltastream DP2 blood pump as an LVAD, we tested the responses of the physiologic controllers to hemodynamic changes and compared them with the response of the constant speed (CS) mode. Both physiologic controllers adapted the pump speed (PS) such that the flow was more sensitive to preload and less sensitive to afterload, as compared with the CS mode. As a result, the risk for suction was strongly reduced. Five suction events were observed in the CS mode, one with the volume-based controller and none with the pressure-based controller. The results suggest that both physiologic controllers have the potential to reduce the number of adverse events when used in the clinical setting.

DOI: https://doi.org/10.1097/MAT.0000000000000533

In Vivo Evaluation of Physiologic Control Algorithms for Left Ventricular Assist Devices Based on Left Ventricular Volume or Pressure

Gregor Ochsner,* Markus J. Wilhelm,† Raffael Amacher,‡ Anastasios Petrou,* Nikola Cesarovic,§ Silvan Staufert,¶ Barbara Röhrnbauer,‡ Francesco Maisano,† Christofer Hierold,¶ Mirko Meboldt,* and Marianne Schmid Daners*

Turbodynamic left ventricular assist devices (LVADs) provide a continuous flow depending on the speed at which the pump is set, and do not adapt to the changing requirements of the patient. The limited adaptation of the pump flow (PF) to the amount of venous return can lead to ventricular suction or overload. Physiologic control may compensate such situations by an automatic adaptation of the PF to the volume status of the left ventricle. We evaluated two physiologic control algorithms in an acute study with eight healthy pigs. Both controllers imitate the Frank–Starling law of the heart and are based on a measurement of the left ventricular volume (LVV) or pressure (LVP), respectively. After implantation of a modified Deltastream DP2 blood pump as an LVAD, we tested the responses of the physiologic controllers to hemodynamic changes and compared them with the response of the constant speed (CS) mode. Both physiologic controllers adapted the pump speed (PS) such that the flow was more sensitive to preload and less sensitive to afterload, as compared with the CS mode. As a result, the risk for suction was strongly reduced. Five suction events were observed in the CS mode, one with the volume-based controller and none with the pressure-based controller. The results suggest that both physiologic controllers have the potential to reduce the number of adverse events when used in the clinical setting. *ASAIO Journal* 2017; 63:568–577.

From the *pd|z Product Development Group Zurich, Department of Mechanical and Process Engineering, ETH Zurich, Zurich, Switzerland; †Department of Cardiovascular Surgery, University Hospital Zurich and University of Zurich, Zurich, Switzerland; ‡Wyss Translational Center Zurich, ETH Zurich and University of Zurich, Zurich, Switzerland; §Division for Surgical Research, University Hospital Zurich and University of Zurich, Zurich, Switzerland; and ¶Micro- and Nanosystems Group, Department of Mechanical and Process Engineering, ETH Zurich, Zurich, Switzerland.

Submitted for consideration september 2016; accepted for publication in revised form january 2017.

Ochsner and Wilhelm are the co-first authors.

Disclosures: The authors have no conflicts of interest to disclose.

Petrou and Staufert have received funding from the Stavros Niarchos Foundation. The study was financially supported by the Institute for Dynamic Systems and Control, ETH Zurich.

Correspondence: Marianne Schmid Daners, pd|z Product Development Group Zurich, Department of Mechanical and Process Engineering, ETH Zurich, CLA G21.1, Tannenstrasse 3, 8092 Zürich, Switzerland. Email: marischm@ethz.ch.

Supplemental digital content is available for this article. Direct URL citations appear in the printed text, and links to the digital files are provided in the HTML and PDF versions of this article on the journal's Web site (www.asaiojournal.com).

DOI: 10.1097/MAT.0000000000000533

Key Words: physiologic control, Frank–Starling law, ventricular assist device

Despite great technical and clinical improvements, left ventricular assist device (LVAD) therapy is still affected by many adverse events like strokes, right ventricular (RV) failure, bleeding, hemolysis, or driveline infection.[1] Some of these adverse events are thought to be promoted by the nonphysiologic response of the LVAD operated at constant speed (CS). However, the direct hemodynamic effects are well understood, the clinical consequences of these are mainly assumptions: when the pump flow (PF) is higher than the blood return to the heart, the LV is emptied by the pump, and eventually, ventricular suction, that is, a collapse of the ventricular walls occurs. Ventricular suction presumably promotes hemolysis and thrombus formation because of flow stasis and damage to the myocardium, which may be sucked onto the pump inlet.[2] In addition, excessive unloading of the LV may lead to a septum shift, which impairs the functioning of the RV and may cause a tricuspid valve insufficiency, which in turn may lead to RV failure.[3] In contrast, when the PF is lower than the blood return and the LV itself is too weak to generate more flow, the LV is overloaded and a congestion of blood in the left atrium (LA) and the pulmonary circulation occurs.[4] Left ventricular overload may additionally injure the already failing LV because of a consecutive increase in wall tension. Furthermore, the increased pulmonary pressure caused by the congestion of blood may, in extreme cases, lead to lung edema and imposes an excessive load on the RV. Physiologic control may have the potential to reduce the number of adverse events by adaptation of the pump speed (PS) and, thus, prevention of suction or overload.

Many physiologic controllers have been analyzed *in silico* or *in vitro* and were presented in the literature, but only few controllers were also tested *in vivo*. The *in vivo* studies can be subdivided into four categories: first, studies which collected *in vivo* data, for example, during a PS ramp, and then proposed a physiologic controller after the analysis of this data.[5–11] Second, studies with suction detection and prevention algorithms.[12–17] Third, studies in which the PS is pulsed in synchrony with the cardiac cycle.[18–24] And fourth, studies with physiologic controllers activated *in vivo* (animals or human patients).[25–30] Of all four categories, only the last represents the case of a closed feedback loop, which is an important difference, because feedback can lead to instability. No chronic *in vivo* experiments with activated physiologic controllers are found in the literature.

We have also presented two physiologic controllers in previous *in vitro* studies: The preload responsive speed (PRS) controller adjusts the PS based on a measurement of the LV volume (LVV),[31]

whereas the systolic pressure (SP) controller adjusts the PS based on a measurement of the LV pressure (LVP).[32] The purpose of both controllers is the imitation of the Frank–Starling law of the heart, which states that the flow generated by the healthy ventricle mainly depends on its preload.[33] The pressure-flow characteristics of a turbodynamic LVAD operated at CS differs greatly from that of a healthy heart. Compared with a healthy LV, the sensitivity of an LVAD to afterload is higher and the sensitivity to preload is lower.[34] This small preload sensitivity is the reason why the adaptation of the PF to the venous return is limited and suction or LV overload can occur. By adapting the PS and indirectly the PF to the preload, the physiologic controllers aim at preventing suction or LV overload and all their negative consequences.

We conducted acute *in vivo* experiments with eight healthy pigs to compare our two physiologic controllers for LVADs with the CS mode. For this purpose, we induced hemodynamic changes, whereas the LVAD was operated in one of the three control modes. Using a heart-lung machine (HLM) and an occlusive balloon catheter placed in the descending aorta, we applied acute pre- and afterload changes and observed changes of the PS, the PF, and multiple hemodynamic variables. The goal of the study was to investigate whether the physiologic controllers react to the induced hemodynamic changes as defined by the Frank–Starling law and whether they work robustly *in vivo*.

Materials and Methods

The experiments were conducted with eight pigs ($m = 91.13 \pm 9.69$ kg). The animal housing and all procedures and protocols were approved by the Cantonal Veterinary Office (Zurich, Switzerland) under the license number 152/2013. Housing and experimental procedures were in accordance with the Swiss animal protection law and also conform to Directive 2010/63 EU of the European Parliament and of the Council of September 22, 2010 on the Protection of Vertebrate Animals used for Experimental and other Scientific Purposes and also conform to the Guide for the Care and Use of Laboratory Animals.

Anesthetic Protocol

After loss of postural reflexes following premedication with ketamine (20 mg/kg), azaperone (1.5 mg/kg), and atropine (0.75 mg), the anesthesia was deepened by a bolus injection of propofol (1–2 mg/kg bodyweight), and the animals were intubated. Anesthesia was then maintained with 2–3% isoflurane and propofol (2–5 mg/kg/h). Amiodarone [2–3 mg/kg bolus intravenously (iv)] was administered as antiarrhythmic therapy in order to stabilize the heart rhythm. Pain management included fentanyl (0.02 mg/kg/h) constant rate infusion (CRI) for the duration of the procedure. After the animals were put on cardio-pulmonary bypass, isoflurane was discontinued and anesthesia was maintained by co-administration of propofol (5 mg/kg/h) and fentanyl (0.02 mg/kg/h) CRI. Vital parameters, reflexes, blood-gases, and acid-base balance were monitored during the whole procedure. After completion of the experimental procedure, the animals were euthanized by an overdose of Na-pentobarbital.

Surgical Procedure

After induction of anesthesia and placement of the animal in supine position, the chest was draped in sterile fashion. Following midline skin incision over the sternum, a median sternotomy was performed. The pericardium was opened. After administration of heparin 300 IE/kg, the aortic arch and right atrium were cannulated (Opti22 OptiSite Arterial Cannula and TFM324L Venous Cannula, Edwards Lifesciences, Irvine, CA) for connection with the HLM (Stöckert SIII, Sorin Group Deutschland GmbH, Munich, Germany). The extracorporeal circulation was started, keeping normothermic conditions. The ascending aorta was completely mobilized for the placement of the flow probe (T-208/24PAU, Transonic Systems, Inc., Ithaca, NY). Three ultrasound crystals (UDG, Sonometrics Corp., London, Canada) were positioned on the LV for volume measurements by using custom-designed, 3D-printed crystal holders. The two short-axis crystals were placed in a midventricular position next to the left anterior descending and posterior descending arteries. One of the long-axis crystals was positioned at the lateral base of the left ventricle, as counterpart for the second long-axis crystal that was attached to the inflow cannula of the LVAD. **Figure 1** illustrates the placement of the crystals, the flow probe, and the HLM tubing.

A modified Deltastream DP2 (Xenios AG, Heilbronn, Germany) extracorporeal blood pump was used as an LVAD. The motor and the controller of the Deltastream DP2 pump were replaced with industrial components (EC 32, maxon motor ag, Sachseln, Switzerland/Accelus ASP-090-09, Copley Controls Corp., Canton, MA), such that the PS could be controlled as desired. An arterial cannula (Opti22 OptiSite) was inserted into the ascending aorta, between flow probe and cannula of the HLM, serving as outflow graft for the LVAD. **Figure 2** shows the inflow cannula that was specifically designed for the experiments and 3D-printed with Polyamide 12 (Materialise NV, Leuven, Belgium). The inflow cannula contains a through-wall recess for a nonmedical grade, digital, barometric pressure sensor KP253 (Infineon Technologies AG, Neubiberg, Germany). The sensing surface of the sensor is in direct contact with the blood flow, whereas the electrical interconnects on the backside were protected by a sealing compound (1-2577 Conformal Coating, Dow Corning Corp., Midland, MI).

For implantation of the LVAD inflow cannula, four felt-supported 3-0 Prolene (Ethicon Inc., Somerville, NJ) U-stitches were placed around the left ventricular apex. After incision of the apex, a muscular cylinder was excised. The inflow cannula was inserted through the apical hole and fixed to the apex by placing the Prolene sutures through the implant ring of the cannula. The outflow and inflow cannulae were connected to the tubing of the LVAD under careful deairing. The LVAD was started at 2,000 rpm and the speed was increased whereas the flow through the HLM was decreased accordingly. A minimal flow of 0.5 L/min was maintained through the HLM to prevent flow stasis. As last step, a pigtail catheter (Ventri-Cath 510 PV Loop Catheter, Millar Instruments Inc., Houston, TX) was inserted through the carotid artery into the LV to measure the LVP, and a Reliant Stent Graft Balloon Catheter (Medtronic, Minneapolis, MN) was placed through the femoral artery into the descending aorta for afterload variations.

Physiologic Controllers

In previous publications, we have presented physiologic control algorithms based on a measurement of the LVV or LVP together with promising *in vitro* results.[31,32] The working

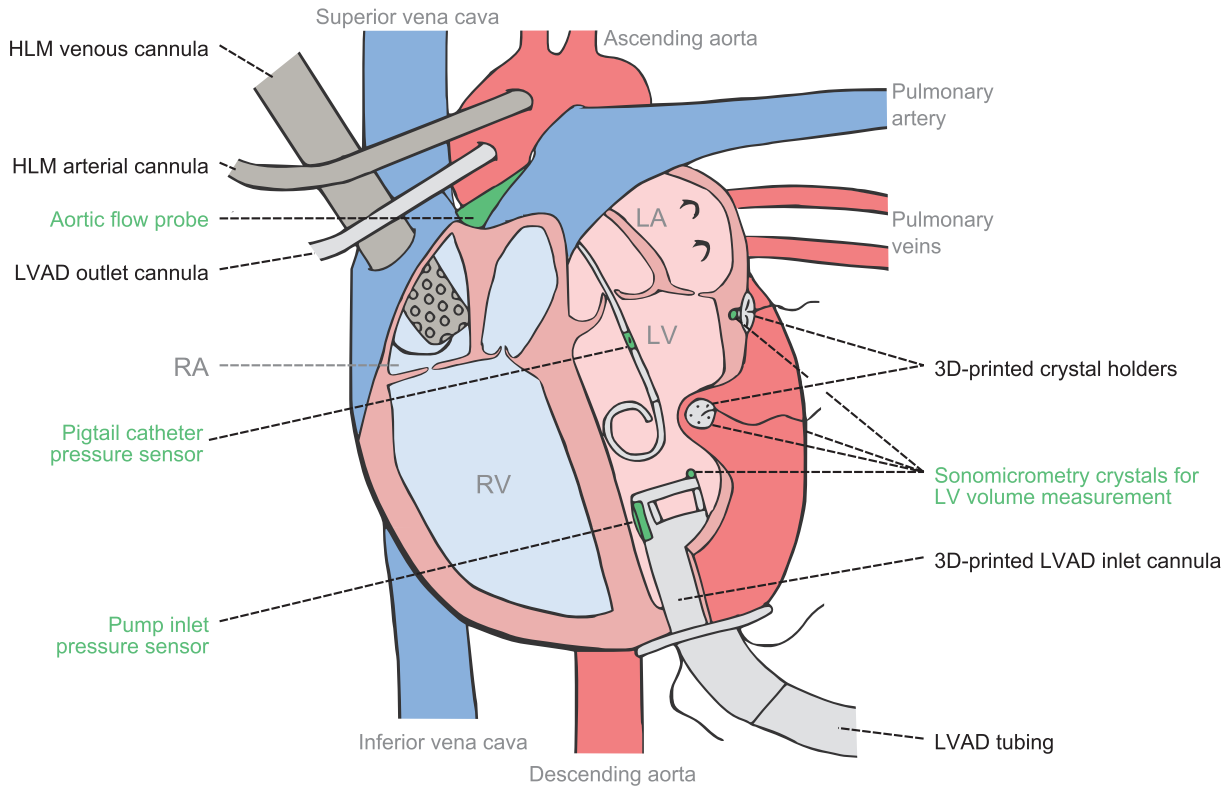

Figure 1. Illustration of the heart with all implanted cannulas and sensors. The four sonomicrometry ultrasound crystals were placed to measure the long and the short axis of the LV. Custom-designed, 3D-printed crystal holders were used to keep three of the crystals fixed in an intramural position; the fourth crystal was placed on the inlet cannula of the LVAD. The pigtail catheter for LVP measurement was used in case the pump inlet pressure sensor failed. LV, left ventricle; LVAD, left ventricular assist device; LVP, LV pressure.

principle of both controllers has been described in detail and is therefore only summarized here. The purpose of both controllers is the imitation of the Frank–Starling law, that is, the adaptation of the PF to the preload of the failing heart.

The PRS controller is operated in the simplified version, where the heart rate is not extracted, but is assumed to be constant at 60 bpm. Five steps are required to compute the desired PS (PS_{des}) based on the measured LVV. First, the LVV signal is low-pass filtered with a second-order infinite impulse response (IIR) filter with bandwidth of 2.7 Hz to remove measurement noise. Second, the end-diastolic volume (EDV) is extracted from the LVV signal by identifying the maximum value from a 1.5 s sliding window. Third, the desired hydraulic power of the pump (PP_{des}) is computed by $PP_{des} = k_{prs} \times (EDV - EDV_0)$, where $k_{prs} = 10$ J/L is the controller gain and the offset EDV_0 is obtained during calibration. Fourth, PS_{des} is computed from PP_{des} using a static, nonlinear mapping, which takes into account the efficiency of the pump and the influence of the cannulae on the resistance to flow. And fifth, the PS_{des} is again low-pass filtered with a first-order IIR filter with a bandwidth of 0.16 Hz.

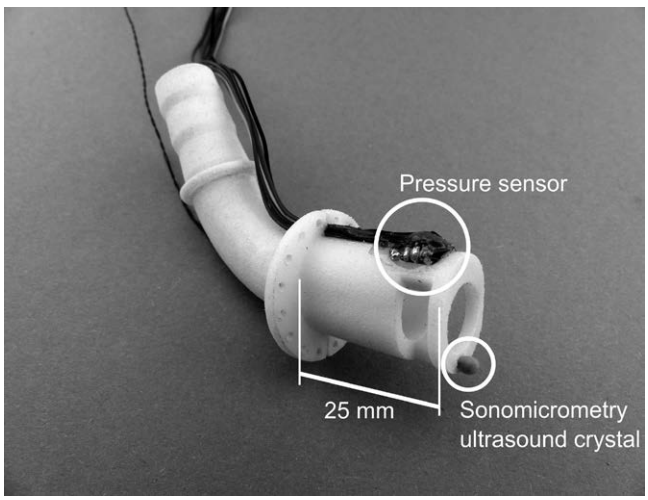

Figure 2. Three-dimensional-printed LVAD inlet cannula with integrated sensors. LVAD, left ventricular assist device.

The SP controller requires four main steps to compute the PS_{des} based on the measured LVP. First, the LVP signal is low-pass filtered with a first-order IIR filter with bandwidth of 15.9 Hz to remove measurement noise. Second, the SP is extracted from the LVP by identifying the maximum value from a 2 s sliding window. Third, PS_{des} is computed by $PS_{des} = k_{sp} \times (SP - SP_0) + PS_0$, where $k_{sp} = 40$ rpm/mm Hg is the controller gain, and the offset SP_0 as well as the reference PS PS_0 are obtained during calibration. And fourth, the PS_{des} is again low-pass filtered with a first-order IIR filter with a bandwidth of 0.32 Hz.

Finally, depending on the selected controller, the respective computed PS_{des} is fed to the speed controller of the electric

motor of the LVAD. Both physiologic controllers were implemented in Matlab/Simulink and executed on Real-Time Windows Target (The MathWorks Inc., Natick, MA).

Experiments

Three different manipulations were applied to simulate hemodynamic changes: a preload reduction, a preload increase, and an afterload increase. The preload was reduced and increased by draining or infusing 500 ml of blood using the HLM. After the preload reduction experiment, the 500 ml were infused back into the pig before another 500 ml were infused to simulate the preload increase. The afterload was increased by inflating the balloon catheter in the descending aorta.

Figure 3 shows an overview of the experimental protocol. With each of the eight pigs, two identical blocks of experiments were conducted (A and B). At the beginning of each block, the volume loading of the pig was adjusted to achieve acceptable flow and pressure levels, and the controllers were calibrated. For the calibration, the pump was set to the CS mode and the speed was manually adjusted such that the mean flow through the aortic valve was approximately 0.5 L/min and no suction occurred. The identified PS was taken as the reference speed for the entire block. Then, both physiologic controllers were automatically calibrated, that is, the parameter EDV_0 of the PRS controller and the parameters SP_0 and PS_0 of the SP controller were set such that PS_{des} of both controllers corresponded to the reference speed identified before. The experiments were then started by randomly selecting one of the three controllers and starting with the first manipulation.

Data Recording and Extraction

Table 1 lists all signals that were recorded continuously at 500 Hz during the experiment. The carotid arterial pressure (CARP) was recorded using the ACQ-7700 System (DSI Ponemah, Valley View, OH); all other signals except the LVP were recorded using an MF624 input/output card (Humusoft s.r.o, Prague, Czech Republic) and Matlab Real-Time Windows Target (The MathWorks Inc.). The signals from the two recording systems were synchronized during postprocessing using a manual trigger signal that was recorded on both systems. Because of its digital interface, the LVP sensor (KP253) was acquired at 200 Hz using an Arduino Due development board (Arduino S.R.L, Scarmagno, Italy), which fed the signal to the PC running Matlab Real-Time Windows Target, where it was upsampled to 500 Hz and recorded. The LVP sensor failed in pigs 2 and 5, and in this case we switched to the pressure measurement of the pigtail catheter as input for the SP controller. Because these two sensors are not placed at the exact same position, they do not measure the same signal. Differences were observed during suction, when the inlet cannula pressure showed negative pressure spikes, but not for the SP that is used as input for the SP controller. The LVV was obtained by measuring the short and long axes of the LV with ultrasound crystals and computing the volume with an ellipsoid model.

Table 1. Recorded Signals

Signal	Abbreviation	Sensor
Left ventricular pressure	LVP	KP253, Infineon Technologies AG, Neubiberg, Germany (pigs 1, 3, 4, 6, 7, and 8) or Ventri-Cath 510 PV Loop Catheter/ MPVS Ultra PV Loop System, Millar Instruments Inc., Houston, TX (pigs 2 and 5)
Carotid arterial pressure	CARP	DTXPlus DT-NN, Argon Medical Devices Inc., Plano, TX
Left ventricular volume	LVV	UDG, Sonometrics Corp., London, Canada
Pump speed	PS	Encoder HEDL 5540, maxon motor ag, Sachseln, Switzerland
Pump flow	PF	TS410/ME-11PXL, Transonic Systems, Inc., Ithaca, NY
Aortic valve flow	AVF	T-208/24PAU, Transonic Systems, Inc., Ithaca, NY

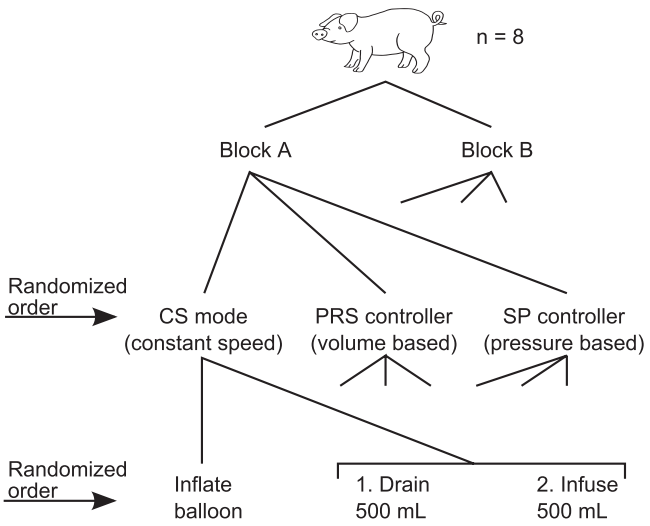

Figure 3. Overview of the study protocol. With all eight pigs, the same experiments were conducted once in block A and once in block B. In each block, both physiologic controllers and the CS mode were tested with all three manipulations, yielding 18 manipulations per pig. The PRS controller is based on LVV; the SP controller is based on LVP. CS, constant speed; LV, left ventricle; LVP, LV pressure; LVV, LV volume; PRS, preload responsive speed; SP, systolic pressure.

For further analysis, steady-state sections before and after each manipulation were extracted. These sections were identified manually and had duration of at least 10 s. The gray-shaded rectangles in **Figure 4** indicate the identified steady-state sections for three preload reduction manipulations. With an automatic algorithm, the individual heartbeats within those sections were identified and beat-by-beat mean values were extracted and stored. From these values, the mean values for the entire section were computed for the following signals: PS, PF, aortic valve flow (AVF), and CARP. The total cardiac output (CO) was computed by adding the mean AVF and PF signals. In addition, the beat-by-beat end-diastolic pressure (EDP) was identified as the pressure on the bottom right corner of the LVP–LVV loop, and the stroke work was extracted by computing the area inside the pressure–volume loop.

Statistical Analysis

For each manipulation (preload reduction, preload increase, and afterload increase) we conducted statistical tests to compare the physiologic controllers with the CS mode of the LVAD. We computed the change in PS (ΔPS) and the change in PF (ΔPF) from before to after the manipulation. Then we used a paired t-test to compare each physiologic controller with the CS mode.

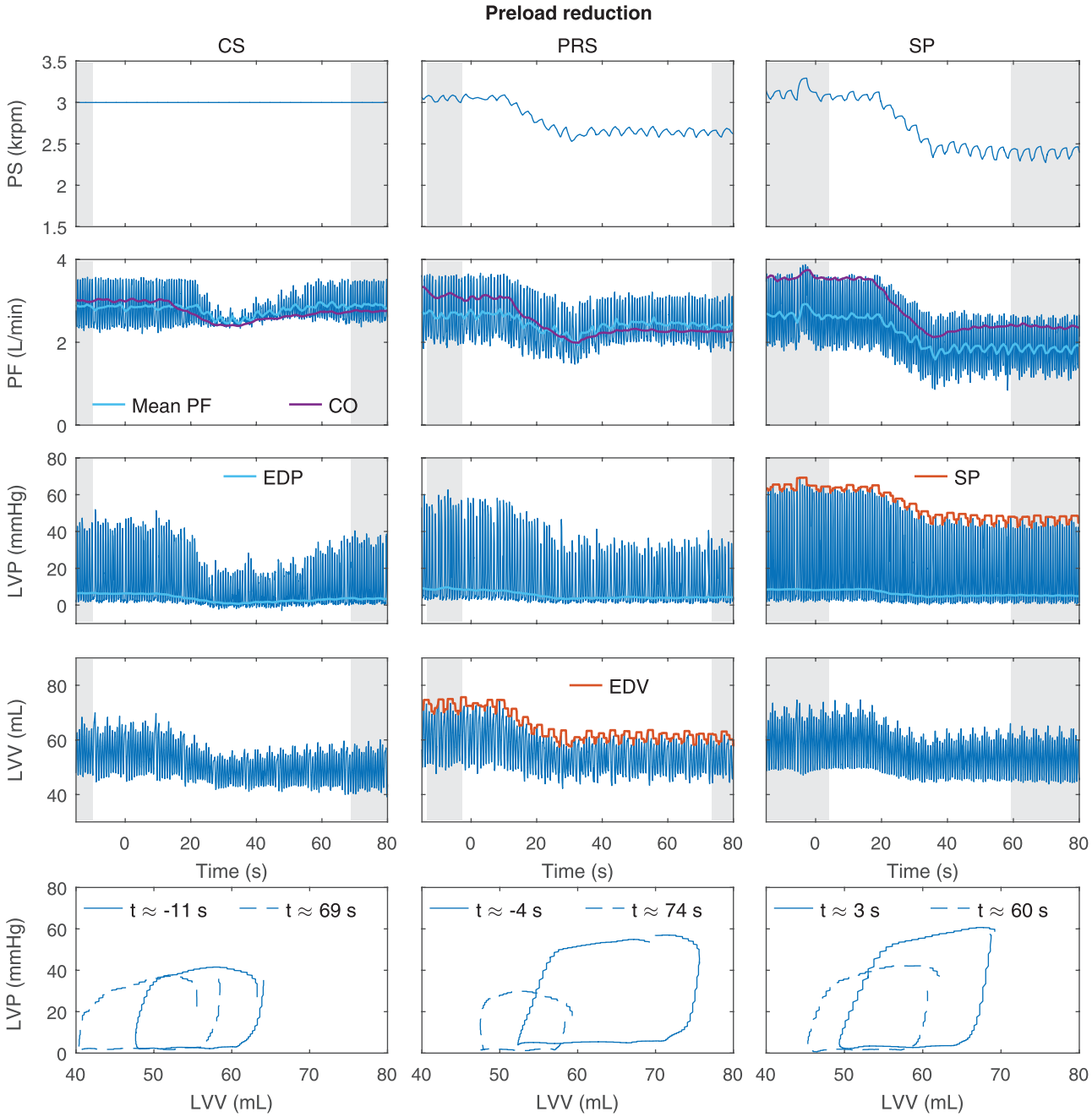

Figure 4. Example results of the preload reduction experiment (pig 5, block A) with the CS mode and both physiologic controllers. The figure shows the PS, the PF, the CO, the LVP, the EDP, and the LVV signals. In addition, the figure depicts pressure–volume loops at steady-state conditions before and after the preload decrease for each control mode. The EDV and the SP signals plotted in red are the respective input signals to the physiologic controllers. The shaded gray areas indicate the steady-state sections that were used to calculate the mean values before and after the manipulations. The preload reduction was started at $t = 0$ s in all three cases. CO, cardiac output; CS, constant speed; EDP, end-diastolic pressure; EDV, end-diastolic volume; LVP, LV pressure; LVV, LV volume; PF, pump flow; PS, pump speed; SP, systolic pressure.

We conducted eight tests per manipulation and applied a Bonferroni correction to counteract the problem of multiple tests, yielding a significance level of $p = 0.05/8 = 0.00625$.

Results

In total, 144 preload and afterload manipulations were planned (18 manipulations in eight pigs) and 139 were conducted completely. The other five manipulations were either not conducted or aborted because of a very low perfusion. Of these 139 manipulations, 19 were excluded, because no steady-state sections could be identified before or after the manipulation. The remaining 120 manipulations were used for further analyses.

Qualitative Analysis of Preload Reduction

Figure 4 shows the results of the preload reduction experiment for pig 5, block A with the CS mode and both physiologic

controllers. The first row shows how both physiologic controllers reduce the PS in response to the reduced preload, whereas it is kept constant in the CS mode. The PF shown in the second row decreases with all three control modes, however, in the CS mode it returns to the initial value after 10 s. The small oscillations in the PS are caused by the mechanical ventilation, which influences the LVP and LVV signals.

Hemodynamics During Preload Reduction

Figure 5 shows the mean values of the PS, the PF, the stroke work, the CO, the EDP, and the CARP before and after the preload reduction experiment from block A for all eight pigs. The purpose of this figure is to show the hemodynamic state of all pigs and the variability between them, as well as the magnitude of the change induced by draining 500 ml of blood. Qualitatively, differences between the CS mode and the physiologic controllers can be observed for the PS and PF signals. When the pump is operated in CS mode, the PS remains constant and the changes in PF are small. With both physiologic controllers, the PS is reduced and the reduction in PF is more pronounced. Quantitative values and a statistical analysis are provided in the subsequent paragraphs. For the stroke work, the CO, the EDP, and the CARP, the qualitative analysis shows no difference between the CS mode and the physiologic controllers. The differences between the two physiologic controllers are also small for all signals and are overshadowed by the inter-animal variability. The results for the preload and afterload increase experiments can be found in the supplementary material (see Supplemental Digital Content, http://links.lww.com/ASAIO/A137), processed in the same manner as the results presented in **Figure 5**.

Statistical Analysis of Pump Speed and Pump Flow

Figure 6 provides a quantitative analysis of the differences between the CS mode and the physiologic controllers with a statistical analysis of the change of the PS and PF signals during the three manipulations. The PS analysis generates five statistically significant results distributed over all manipulations and both controllers. The p value of all comparisons is small and all speed changes except of one (afterload increase, SP controller, block A) go in the expected direction. Three PF comparisons are statistically significant; none of them for the preload

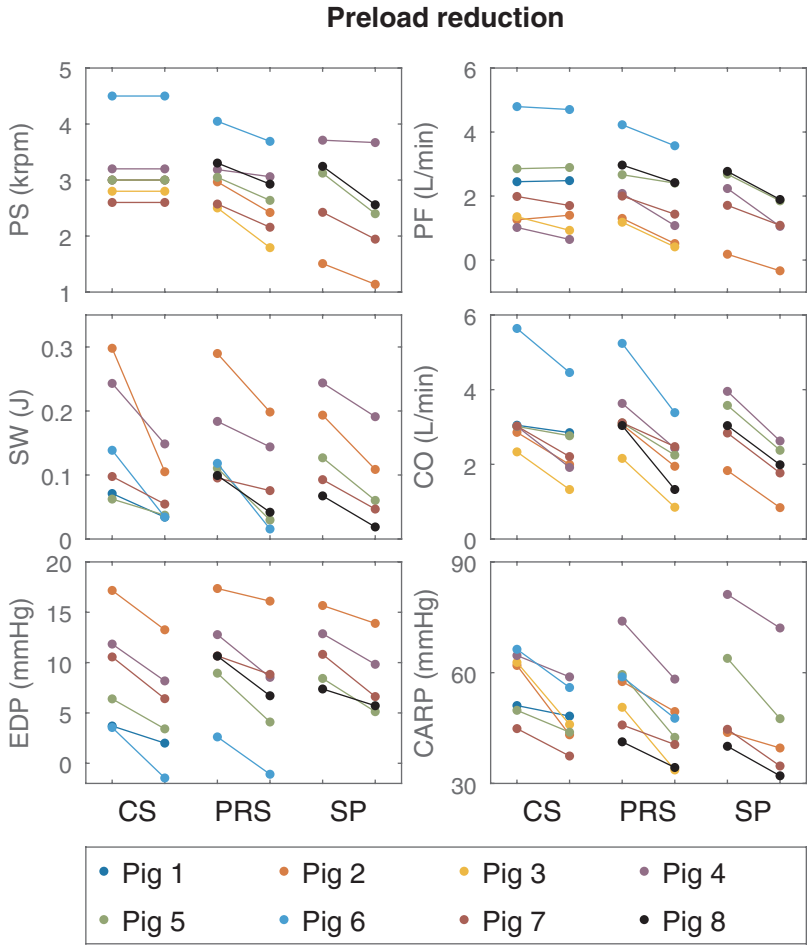

Figure 5. Hemodynamic changes during the preload reduction experiment for block A and all eight pigs. Each panel shows the change of one signal for the CS mode on the left hand side, the PRS controller in the middle, and the SP controller on the right hand side. The figure shows six signals: the PS, the PF, the SW, the CO, the EDP, and the CARP. Same figures but for pre- and afterload increase experiments can be found in the supplementary material (see Supplemental Digital Content, http://links.lww.com/ASAIO/A137). CARP, carotid arterial pressure; CO, cardiac output; CS, constant speed; EDP, end-diastolic pressure; PF, pump flow; PRS, preload responsive speed; PS, pump speed; SP, systolic pressure; SW, stroke work.

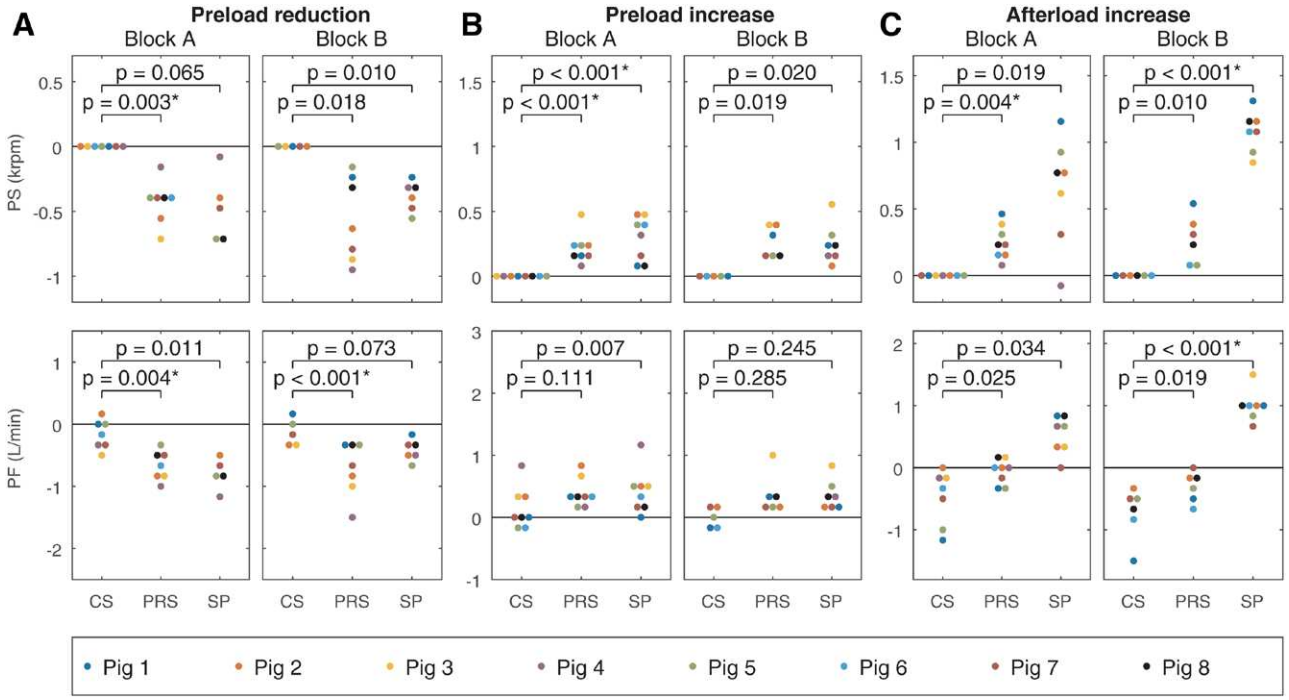

Figure 6. Change of the PS (ΔPS) and PF (ΔPF) during the preload reduction, the preload increase, and the afterload increase experiments. The values of the PRS and the SP controllers were compared with the values obtained with the CS mode using a paired t-test with a significance level of 0.00625. CS, constant speed; PRS, preload responsive speed; SP, systolic pressure.

increase manipulation. **Table 2** lists the mean and standard deviation of ΔPS and ΔPF over both blocks for each manipulation and each control mode. Although both controllers react similarly to preload changes, the reaction of the SP controller to the afterload increase is stronger.

Preload Sensitivity

In order to investigate whether the reaction of the two controllers to the preload changes is appropriate, we extracted the preload sensitivity of the LVAD as the change in PF divided by the change in preload ΔPF/ΔEDP. A physiologic preload sensitivity value is reported by Salamonsen *et al.*[34] as 0.21 ± 0.03 L/min/mm Hg. The values we obtained from the preload reduction experiment are 0.03 ± 0.08 L/min/mm Hg for the CS mode, 0.21 ± 0.29 L/min/mm Hg for the PRS controller, and 0.26 ± 0.13 L/min/mm Hg for the SP controller.

Ventricular Suction

In total, 34 preload reduction experiments were conducted with the pump inlet pressure sensor active and ventricular suction was observed six times: five times with the CS mode and once with the PRS controller. **Table 3** lists all suction cases to provide an overview of the hemodynamic conditions that prevailed before the preload reduction experiments were started. During suction, all signals were highly transient and no steady-state phase could be identified. Two cases can also be found in **Figure 5**, but the corresponding steady-state sections were identified after the suction events.

Discussion

The study results show clearly that both the PRS controller as well as the SP controller react to preload changes in the expected direction and thereby imitate the Frank–Starling law of the heart. **Figure 6A, B** shows that in response to a preload reduction (increase), both controllers reduce (increase) the PS, resulting in a reduced (increased) PF. The question whether the reaction is adequately strong is answered with the preload sensitivity values listed in the Results section paragraph titled Preload Sensitivity. Although these numbers are affected by a high variance, they indicate that the preload sensitivity of the controllers is similar to that of the native heart. The reaction of the controllers to the preload increase is weaker than that to the preload reduction (**Table 2**). We believe that this difference can be explained by the high contractility of the healthy

Table 2. Mean and Standard Deviation Over Both Blocks

	CS Mode		PRS Controller		SP Controller	
Manipulation	ΔPS (rpm)	ΔPF (L/min)	ΔPS (rpm)	ΔPF (L/min)	ΔPS (rpm)	ΔPF (L/min)
Preload reduction	0	−0.13 ± 0.21	−496 ± 265	−0.68 ± 0.35	−408 ± 198	−0.60 ± 0.28
Preload increase	0	0.10 ± 0.29	241 ± 104	0.36 ± 0.26	279 ± 146	0.39 ± 0.29
Afterload increase	0	−0.57 ± 0.45	263 ± 149	−0.17 ± 0.25	860 ± 373	0.74 ± 0.39

CS, constant speed; PF, pump flow; PRS, preload responsive speed; PS, pump speed; SP, systolic pressure.

Table 3. Suction Cases

Case	Control Mode	Pig	Block	PF Before Suction (L/min)	End-Diastolic Pressure Before Suction (mm Hg)	Duration of Suction (s)
1*	CS	3	A	1.35	n/a†	5
2	CS	3	B	1.24	n/a†	6
3	CS	4	B	2.21	12.37	7‡
4*	PRS	6	A	4.23	2.62	2
5	CS	8	A	2.94	7.56	9
6	CS	8	B	2.75	10.22	5

*These experiment can be found in **Figure 5**.
†EDP could not be extracted reliably for pig 3 because of the round shape of the pV loop.
‡Then aborted and volume reinfused.
CS, constant speed; PF, pump flow; PRS, preload responsive speed.

LV, which can fully compensate for the preload increase by increasing the AVF, which in turn prevents the controllers to increase the PF substantially. A categorization of the two controllers in comparison with others presented in literature can be found in a previous publication.[32]

Most physiologic controllers are designed to prevent suction; however, their reaction can be too weak or too slow such that suction may still occur. The findings of this study suggest that our physiologic controllers are able to prevent suction effectively. The one suction event observed with the PRS controller was released after only two heartbeats, which indicates that the controller did not fail completely in this case. For a clinical application, the physiologic controllers will be extended by an additional suction detection system as proposed in the literature.[14] In addition, a similar system would intervene when the PS is very low or very high over a longer time, indicating sensor drift or a similar malfunction. However, in the current study we only tested the core algorithm of the control system.

The results of the current study show that the PRS controller also reacts to afterload changes in the expected manner, that is, as defined by the Frank–Starling law. **Figure 6C** shows that when the afterload is increased, the PRS controller increases the PS to counteract the decrease in PF. The question whether the reaction is adequately strong is easier to answer compared with the preload reduction, because we want the PF to be insensitive to afterload. With the PRS controller, this goal is achieved, as the change in PF almost goes to zero (ΔPF = -0.17 ± 0.25 L/min) compared with -0.57 ± 0.45 L/min with the CS mode. In contrast, the reaction of the SP controller to an afterload increase is too strong, which results in an increase in PF by 0.74 ± 0.39 L/min. This overreaction is clearly undesirable as it may lead to excessive arterial pressures. However, previous *in vitro* studies have shown that with a weak LV and under LVAD support, the SP is less influenced by the afterload.[32] We therefore assume that with a failing instead of a healthy LV, the reaction of the SP controller to afterload changes would be more adequate. In general, it remains to be determined whether the imitation of the Frank–Starling law without taking the perfusion into account explicitly represents the optimal physiologic control system.

One important outcome of this study is the proof of the robustness of both physiologic controllers: No experiment had to be aborted because of a controller problem. In fact, we conducted two identical blocks of experiments (A and B) with each pig and did not observe any substantially different results. The sensors we used to measure the LVV and LVP can only be used for acute experiments, but they proved to be sufficiently accurate, that is, the accuracy requirements for future biocompatible sensor systems are moderate. Clearly, the development of reliable, long-term stable implantable sensors is absolutely critical for the success of physiologic control. Before the second block, we recalibrated both physiologic controllers. This procedure was necessary, because the hemodynamics changed continuously and the controller settings rendered inappropriate after some time. Whereas the hemodynamic changes during an acute experiment are presumably different from those observed in LVAD patients, a chronic study with a physiologic controller is required to answer the question of how much recalibration is required. Both physiologic controllers also worked well during arrhythmic periods, which were observed in two of the eight pigs.

The controller gains need to be selected carefully as a compromise between performance and stability. When the gains are too low, the difference to the CS mode is negligible; when the gains are too high the controllers can become unstable. Both controller gain values were selected based on *in vitro* experiments. The gain of the PRS controller additionally allows a physiologic interpretation as the slope of the preload recruitable stroke work.[31,32] In preliminary *in vivo* experiments, we had tested higher and lower gain values. Sustained oscillations could be observed with gain values around $k_{prs} = 20$ J/L and $k_{sp} = 80$ rpm/mm Hg, which indicates that the stability margins with the normal gains are approximately 2. With low gains, that is, $k_{prs} = 5$ J/L and $k_{sp} = 20$ rpm/mm Hg, no substantial difference to the CS mode could be observed. Therefore, we believe that the presented values represent a reasonable compromise between a high gain margin and a good preload sensitivity.

Although the current study shows that the reaction of the controllers is physiologic, it does not allow a statement on their effectiveness in human patients. The results in **Figure 5** show that the stroke work, the CO, the EDP, and the CARP are all not substantially affected by the presence of physiologic control. This outcome can be well explained by the healthy pig model that was used. Only Schima *et al*.[29] have tested a physiologic controller in human patients and they reported a significant increase in PF and significant decrease in pulmonary arterial pressure in response to physical exercise. The PRS and the SP controller are expected to achieve a similar response in human patients. However, although those results show that physiologic control can improve the hemodynamics, only long-term clinical experience will show whether the number of adverse events can be reduced.

Limitations

The main limitation of the presented study is the use of a healthy animal model. Because of the high contractility of the healthy LV, the preload sensitivity of the combined heart-LVAD system was very high. Consequently, the hemodynamics of our model differs substantially from those of a patient suffering from heart failure. However, both physiologic controllers have already been evaluated *in vitro* with a HF model.[31,32] We expect a similar behavior of the controllers in a HF animal model. Furthermore, this study represents the first approach to test the two physiologic controllers *in vivo* and because of the complexity, we decided not to use pharmacological agents to reduce the contractility or to alter the afterload. Future studies, however, will have to be conducted with a heart failure animal model that is more complex but represents the clinical situation more accurately.

Another limitation concerns the LVP and LVV sensors we used. Not only the ellipsoid model, but also the placement of the sonomicrometry ultrasound crystals introduced uncertainty on the measured LVV. However, the offset of the LVV had no influence on the closed-loop system with the PRS controller. Furthermore, the lack of long-term stability of both pressure and volume sensors constitutes a yet unsolved problem, which hampers the chronic *in vivo* or even clinical implementation of physiologic control. Nevertheless, both sensors served for the purpose of the study, that is, for deriving short-term recordings during the acute animal trials and, eventually, evaluating the physiologic controllers.

Conclusion

This study shows that both the PRS controller as well as the SP controller work robustly *in vivo* and adapt the PF according to the Frank–Starling law of the heart, which strongly reduces the risk of ventricular suction or overload.

The effectiveness of the two controllers in reacting to hemodynamic changes is promising. Integrated in an LVAD, they may be able to fulfill the needs of physiologic adaptation in the clinical setting. Future work is necessary to develop completely integrated, long-term stable and biocompatible sensor systems feeding the controller with the required LVV or LVP signal.

Acknowledgment

The authors thank Stefan Boës for the design of the 3D-printed crystal holders, Prof. Dominik Obrist for lending us the aortic flow probe, and Prof. Burkhardt Seifert for his statistical advice. In addition, the authors thank Stefan Kolb from Infineon Technologies for providing pressure sensors, and the team of veterinaries and perfusionists at the University Hospital Zurich, without whom the experiments would not have been possible. This work is part of the Zurich Heart project under the umbrella of University Medicine Zurich.

References

1. Kirklin JK, Naftel DC, Pagani FD, *et al*: Seventh INTERMACS annual report: 15,000 patients and counting. *J Heart Lung Transplant* 34: 1495–1504, 2015.
2. Reesink K, Dekker A, Van der Nagel T, *et al*: Suction due to left ventricular assist: Implications for device control and management. *Artif Organs* 31: 542–549, 2007.
3. Vollkron M, Schima H, Huber L, Wieselthaler G: Interaction of the cardiovascular system with an implanted rotary assist device: Simulation study with a refined computer model. *Artif Organs* 26: 349–359, 2002.
4. AlOmari AH, Savkin AV, Stevens M, *et al*: Developments in control systems for rotary left ventricular assist devices for heart failure patients: A review. *Physiol Meas* 34: R1–27, 2013.
5. Boston JR, Antaki JF, Simaan MA: Hierarchical control of heart-assist devices. *IEEE T Robotic Autom* 10: 54–64, 2003.
6. Gwak KW, Antaki JF, Paden BE, Kang B: Safety-enhanced optimal control of turbodynamic blood pumps. *Artif Organs* 35: 725–732, 2011.
7. Jansen-Park SH, Spiliopoulos S, Deng H, *et al*: A monitoring and physiological control system for determining aortic valve closing with a ventricular assist device. *Eur J Cardiothorac Surg* 2014;46:356–360.
8. Konishi H, Antaki JF, Amin DV, *et al*: Controller for an axial flow blood pump. *Artif Organs* 20: 618–620, 1996.
9. Ohuchi K, Kikugawa D, Takahashi K, *et al*: Control strategy for rotary blood pumps. *Artif Organs* 25: 366–370, 2001.
10. Oshikawa M, Araki K, Endo G, Anai H, Sato M: Sensorless controlling method for a continuous flow left ventricular assist device. *Artif Organs* 24: 600–605, 2000.
11. Salamonsen RF, Pellegrino V, Fraser JF, *et al*: Exercise studies in patients with rotary blood pumps: Cause, effects, and implications for starling-like control of changes in pump flow. *Artif Organs* 37: 695–703, 2013.
12. Mason DG, Hilton AK, Salamonsen RF: Reliable suction detection for patients with rotary blood pumps. *ASAIO J* 54: 359–366, 2008.
13. Voigt O, Benkowski RJ, Morello GF: Suction detection for the MicroMed DeBakey left ventricular assist device. *ASAIO J* 51: 321–328, 2005.
14. Vollkron M, Schima H, Huber L, Benkowski R, Morello G, Wieselthaler G: Advanced suction detection for an axial flow pump. *Artif Organs* 30: 665–670, 2006.
15. Salamonsen RF, Lim E, Moloney J, Lovell NH, Rosenfeldt FL: Anatomy and physiology of left ventricular suction induced by rotary blood pumps. *Artif Organs* 39: 681–690, 2015.
16. Wang Y, Simaan MA: A suction detection system for rotary blood pumps based on the Lagrangian support vector machine algorithm. *IEEE J Biomed Health Inform* 17: 654–663, 2013.
17. Yuhki A, Hatoh E, Nogawa M, Miura M, Shimazaki Y, Takatani S: Detection of suction and regurgitation of the implantable centrifugal pump based on the motor current waveform analysis and its application to optimization of pump flow. *Artif Organs* 23: 532–537, 1999.
18. Ando M, Takewa Y, Nishimura T, *et al*: A novel counterpulsation mode of rotary left ventricular assist devices can enhance myocardial perfusion. *J Artif Organs* 14: 185–191, 2011.
19. Arakawa M, Nishimura T, Takewa Y, *et al*: Novel control system to prevent right ventricular failure induced by rotary blood pump. *J Artif Organs* 17: 135–141, 2014.
20. Kishimoto Y, Takewa Y, Arakawa M, *et al*: Development of a novel drive mode to prevent aortic insufficiency during continuous-flow LVAD support by synchronizing rotational speed with heartbeat. *J Artif Organs* 16: 129–137, 2013.
21. Pirbodaghi T, Weber A, Axiak S, Carrel T, Vandenberghe S: Asymmetric speed modulation of a rotary blood pump affects ventricular unloading. *Eur J Cardiothorac Surg* 43: 383–388, 2013.
22. Soucy KG, Giridharan GA, Choi Y, *et al*: Rotary pump speed modulation for generating pulsatile flow and phasic left ventricular volume unloading in a bovine model of chronic ischemic heart failure. *J Heart Lung Transplant* 34: 122–131, 2015.
23. Tuzun E, Chorpenning K, Liu MQ, *et al*: The effects of continuous and intermittent reduced speed modes on renal and intestinal perfusion in an ovine model. *ASAIO J* 60: 19–24, 2014.
24. Umeki A, Nishimura T, Takewa Y, *et al*: Change in myocardial oxygen consumption employing continuous-flow LVAD with cardiac beat synchronizing system, in acute ischemic heart failure models. *J Artif Organs* 16: 119–128, 2013.
25. Choi S, Antaki JF, Boston JR, Thomas D. A sensorless approach to control of a turbodynamic left ventricular assist system. *IEEE T Contr Syst T* 9: 473–482, 2001.
26. Gregory SD, Stevens MC, Pauls JP, *et al*: *In Vivo* evaluation of active and passive physiological control systems for rotary left and right ventricular assist devices. *Artif Organs* 40: 894–903, 2016.

27. Gwak KW: Application of extremum seeking control to turbodynamic blood pumps. *ASAIO J* 53: 403–409, 2007.
28. Olegario PS, Yoshizawa M, Tanaka A, *et al*: Outflow control for avoiding atrial suction in a continuous flow total artificial heart. *Artif Organs* 27: 92–98, 2003.
29. Schima H, Vollkron M, Jantsch U, *et al*: First clinical experience with an automatic control system for rotary blood pumps during ergometry and right-heart catheterization. *J Heart Lung Transplant* 25: 167–173, 2006.
30. Vollkron M, Schima H, Huber L, Benkowski R, Morello G, Wieselthaler G: Development of a reliable automatic speed control system for rotary blood pumps. *J Heart Lung Transplant* 24: 1878–1885, 2005.
31. Ochsner G, Amacher R, Wilhelm MJ, *et al*: A physiological controller for turbodynamic ventricular assist devices based on a measurement of the left ventricular volume. *Artif Organs* 38: 527–538, 2014.
32. Petrou A, Ochsner G, Amacher R, *et al*: A Physiological controller for turbodynamic ventricular assist devices based on left ventricular systolic pressure. *Artif Organs* 40: 842–855, 2016.
33. Guyton AC, Hall JE. *Textbook of Medical Physiology*, 12th ed. Philadelphia, Saunders, 2010.
34. Salamonsen RF, Mason DG, Ayre PJ: Response of rotary blood pumps to changes in preload and afterload at a fixed speed setting are unphysiological when compared with the natural heart. *Artif Organs* 35: E47–E53, 2011.